Hindawi Publishing Corporation
EURASIP Journal on Wireless Communications and Networking
Volume 2009, Article ID 467315, 15 pages
doi:10.1155/2009/467315

Research Article

Achievable Throughput-Based MAC Layer Handoff in IEEE 802.11 Wireless Local Area Networks

SungHoon Seo,[1] JooSeok Song,[1] Haitao Wu,[2] and Yongguang Zhang[2]

[1] *Department of Computer Science, Yonsei University, Seoul 120-749, South Korea*
[2] *Wireless and Networking Group, Microsoft Research Asia, Beijing 100190, China*

Correspondence should be addressed to SungHoon Seo, hoon@emerald.yonsei.ac.kr

Received 27 March 2009; Accepted 10 June 2009

Recommended by Naveen Chilamkurti

We propose a MAC layer handoff mechanism for IEEE 802.11 Wireless Local Area Networks (WLAN) to give benefit to bandwidth-greedy applications at STAs. The proposed mechanism determines an optimal AP with the maximum achievable throughput rather than the best signal condition by estimating the AP's bandwidth with a new on-the-fly measurement method, Transient Frame Capture (TFC), and predicting the actual throughput could be achieved at STAs. Since the TFC is employed based on the promiscuous mode of WLAN NIC, STAs can avoid the service degradation through the current associated AP. In addition, the proposed mechanism is a client-only solution which does not require any modification of network protocol on APs. To evaluate the performance of the proposed mechanism, we develop an analytic model to estimate reliable and accurate bandwidth of the AP and demonstrate through testbed measurement with various experimental study methods. We also validate the fairness of the proposed mechanism through simulation studies.

1. Introduction

As wireless networking grows in popularity, various radio access technologies have been developed to provide better environment for user data service. Most of all, IEEE 802.11 Wireless Local Area Network (WLAN) is one of the dominant wireless technologies to support high-speed network access nowadays. The WLAN basically forms an infrastructure with two network components, Access Point (AP) and Station (STA). An AP is generally distributed at a fixed location, and the WLAN infrastructure connects STAs to a wired network via the AP within their communication range. AP's signal range is denoted by Basic Service Set (BSS) or hotspot which generally provides coverage within a few ten-meter radius.

In large scale wireless networks, multiple APs are densely deployed, and their hotspot ranges are overlapped in the vicinity of one another (e.g., campus, building, and airport lounge) with different types of physical (PHY) standard and channel frequency. Each PHY standard provides various channel modulation rate (e.g., 1, 2, 5.5, 11 Mbps for 802.11b and 6, 12, 24 Mbps for 802.11a); thus the performance may differ in accordance with AP configuration setting. Also, each AP can be configured with a different channel; thus adjacent APs with orthogonal frequencies (e.g., 1, 6, and 11 in 802.11b) are recommended to avoid interchannel interference which causes the disruption of signal quality and channel utilization [1].

Due to the nature of 802.11, an STA can associate with only an AP at a time through a channel assigned on the AP; thus at the same time the STA cannot listen to any signal from APs operated on the other channels. In order to listen to signals from other channel APs, STAs should switch their channel, but it may cause the blocking of on-going communication through their current associated AP. Even if STAs can listen to beacon frames from other APs operated on the same channel, it is limited only when their listen period and the APs' beacon interval are exactly matched. This is because the 802.11 STAs repeat to change their Network Interface Card (NIC) mode in sleeping and listening to beacon frame for Power Saving.

When the signal condition from the current associated AP becomes poor to communicate, STAs should discover other APs and continue the communication by performing

a MAC layer handoff. For the discovery, STAs perform *active scanning* by broadcasting a special management frame, that is, Probe Request, to every channel supported by their NIC. An STA triggers the *active scanning* when the Received Signal Strength Index (RSSI) of the current associated AP is below the predefined threshold (usually about −90 dBm), and the STA builds the list of the AP available to itself. Then, the STA performs handoff to an AP whose signal condition is better than the current associated AP, mainly based on the RSSI as in [2, 3]. However, using the RSSI as a criterion to perform handoff is not good enough because the RSSI itself does not mean the AP's capability information.

Therefore we propose a MAC layer handoff mechanism for IEEE 802.11 WLAN by using AP's capability information as a handoff criterion, especially an achievable throughput from APs. To estimate the achievable throughput, we devise a new method, namely, Transient Frame Capture (TFC). The TFC works with the promiscuous mode of WLAN NIC so that STAs can keep their connections through the current associated AP without service degradation. The proposed handoff mechanism allows STAs to determine an optimal AP whose bandwidth satisfies the requirement of applications at the STAs, thus gives the most benefit to the STAs when performing the handoff. We develop an analytic model and demonstrate through testbed measurements with various experimental study methods to show the effects on reliability and accuracy of the throughput estimation. Furthermore, we perform simulation studies to validate the proposed mechanism in regard to the fairness of APs. Especially, this paper contributes in the following four aspects.

(1) We provide a client-only solution for the achievable throughput-based handoff mechanism so that it does not require any modifications or changes on AP's protocol and configuration. That is, it works with any existing setup of already deployed WLAN infrastructure.

(2) We devise a new method to estimate the actual bandwidth capacity as well as the achievable throughput from neighbor APs without service degradation through the current associated AP.

(3) From a view point of AP deployment, the traffic load on multiple APs should be fairly distributed. The proposed handoff mechanism enables STAs to select the most bandwidth-beneficial AP. This also gives an advantage of balancing the load on the different types of APs.

(4) Our implementation and experimental studies are the first attempt to address AP's throughput measurement only from the STA side. Also, the measurement estimates near the boundary of the actual throughput in the 802.11 environments.

The rest of this paper is organized as follows. Section 2 introduces background on MAC layer handoff and bandwidth estimation. In Section 3, we describe the proposed handoff mechanism which is the basis of achievable throughput. Section 4 provides details of TFC algorithm, and Section 5 presents the analytic model to estimate the achievable throughput. In Section 6, we show the evaluation of the proposed mechanism through experiment and simulation studies, and Section 7 concludes this paper.

2. Related Work and Motivation

The IEEE 802.11 MAC layer handoff procedure is split into trigger, discovery, AP selection, and commitment (Throughout this paper, the MAC layer handoff is alternatively used for the term "layer 2 handoff" or "L2 handoff"). The most of previous researches [2–4] are based on the RSSI measured from current associated AP as a criterion not only to trigger handoff but also to select optimal AP. After an STA triggers handoff, it discovers neighbor APs and channels available to itself with active scanning to all channels supported by its WLAN NIC which causes the major portion of the entire handoff latency. Even if authors of [3, 5] proposed solutions to reduce the latency, they have limitations of a difficulty to modify already deployed AP software and ineffective cost to equip additional scanning purpose NIC at the STA. The AP selection procedure is also based on the RSSI so that STAs perform handoff to an AP with the maximum RSSI. Wu et al. [4] proposed an RSSI-based AP selection mechanism to reduce the handoff latency and to avoid service degradation of VoIP traffic. However, RSSI itself does not indicate the AP's capability (e.g., achievable bandwidth); thus the STA may suffer the severe degradation of on-going service after performing the handoff to a highly loaded AP.

Bandwidth estimation has been a hot research topic and mainly addressed by using packet dispersion [6]. The packet dispersion was originally designed to estimate end-to-end bandwidth on wired network environment where cross traffic exists along with the intermediate nodes in the routing path. However, the packet dispersion over- or under-estimates the bandwidth on the wireless network environment; thus a few research [7–12] has been investigated to estimate accurate bandwidth for the wireless environment. References [7, 8] provided solutions to estimate the saturated and the potential bandwidth on AP by analyzing the distribution of packet delay and beacon frames. In [9], Li et al. attempted to use the packet dispersion in the 802.11 WLAN by analyzing the channel access time. Also, as a passive manner, [10–12] presented solutions to estimate bandwidth on AP by analyzing channel occupation probability. However, these methods mainly focused on the bandwidth measurement itself by actively sending probes to the AP or passively receiving beacons from the AP (one-way measurement); thus they are not applicable methods as a client-only solution which limits the protocol changes at APs.

Most recently, Kandula et al. [13] proposed a client-only solution to maximize user throughput based on the available bandwidth measurement by switching channel between multiple APs. To increase the user throughput, the solution virtually maintains multiple IP flows mapped with WLAN NIC's duplicated MAC addresses. However, it cannot maintain a single flow (e.g., UDP-based application) separately through multiple APs because the throughput gain

depends on the number of flows. Moreover, STAs should always maintain connections and monitor actual packets through multiple APs to measure available bandwidth. It means that the solution may degrade the entire channel utilization since STAs should be fully connected to the multiple APs whether they are used for communication or not.

2.1. Problem Statement—The Motivation. As mentioned earlier, most of L2 handoff mechanisms addressed RSSI as a handoff criterion but the RSSI itself does not indicate the actual capability of APs. If an STA has the knowledge of AP's capability information (i.e., achievable throughput after the STA handoff to the AP), it can help the STA to determine a better AP which provides higher throughput to the STA. Even if IEEE 802.11e [14] provides a capability information, the number of STA associated with the AP, this information is not enough to estimate the AP's current bandwidth occupied by active STAs. New radio resource measurements for WLAN are defined in IEEE 802.11k [15], and how meaningful data can be collected through the measurements is discussed in [16]. The 802.11k enables STAs to request measurements (e.g., channel occupation rate) from other STAs (or APs), but it requires the protocol modification of both STAs and APs. Furthermore, measurement frames either on the operating or nonoperating channel affect the on-going traffic thus they may increase the signaling overhead which causes the interruption of data services.

Figure 1 illustrates a scenario that an STA moves across the overlapped hotspots, BSS1 and BSS2, with two APs, where each hotspot is configured with a different channel number (1 and 149). In the BSS1, the STA has associated with current AP (cAP) which supports 802.11b. The STA's RSSI from the cAP is very high (−45 dBm), but the bandwidth loaded on the cAP is relatively higher because other n STAs are activated through the cAP in the BSS1 (e.g., 4 STAs, from STA 1 to STA 4, each of these individually occupies about 1 Mbps bandwidth on the cAP). On the other hand, in the BSS2, a neighbor AP (nAP) supports 802.11a. Relatively lower RSSI of the nAP is acceptable for the STA to associate, but the traffic load on the nAP is lower than that on the cAP (<1 Mbps). If the STA associates with the nAP even in lower RSSI, it is beneficial for the STA to achieve higher bandwidth through the nAP.

In this sense, using the RSSI as a handoff criterion in the conventional MAC layer handoff mechanism is not good enough to give more benefit to bandwidth-greedy applications (such as FTP, P2P file sharing, and e-mail) which require bandwidth as high as possible. We therefore take the achievable throughput from APs available to STAs into account the main criterion of the proposed handoff mechanism. By utilizing newly devised method, Transient Frame Capture (TFC), STAs not only estimate bandwidth capacity but also predict the achievable throughput from the target AP (as denoted by nAP in Figure 1). Since the TFC is performed in a very short time with fast channel switching, STAs do not suffer from the service degradation through the cAP even occurring retransmissions caused by frame loss and delayed ACK transmission. Moreover, the TFC is passively conducted under the promiscuous mode operation of NIC; it thus affects no interference to other contending STAs within the same channel BSS. With the result of the TFC, STAs can perform handoff to an optimal AP which guarantees the maximum achievable throughput to the STAs.

3. The Proposed MAC Layer Handoff Mechanism

In this section we describe the details of the proposed MAC layer handoff mechanism which addresses the achievable throughput as a handoff criterion rather than the RSSI. A newly devised TFC method enables STAs to estimate the bandwidth capacity and to predict the achievable throughput of neighbor APs. Since no guarantee STAs will be able to achieve similar performance due to asymmetric fading, we further investigate how wireless condition affects the predicted achievable throughput according to the link quality such as RSSI and Frame Error Rate (FER).

We summarize the procedure for our handoff mechanism as follows.

(1) The proposed handoff is triggered.

(2) Build a BSS list for neighbor APs available to the STA. We assume that this step can be actively performed by channel scanning as in [4].

(3) Capture 802.11 frames on the BSS of neighbor APs (appeared in the BSS list) by utilizing Transient Frame Capture.

(4) Estimate the achievable throughput from each of the APs by analyzing the captured frame information.

(5) Select an optimal AP with the maximum achievable throughput and perform handoff to the AP.

3.1. AP Selection Algorithm. STAs should select a target AP before they perform a handoff. We use an achievable throughput as a metric to determine an optimal target AP among neighbor APs. The AP selection for the proposed handoff mechanism is conducted with an algorithm as follows. Once an STA finds neighbor APs with a scan method as introduced in [4], it builds a BSS list for every neighbor AP. Let U denote a set of every neighbor AP in the BSS list, and it is given by $U = \{\mathrm{AP}_1, \mathrm{AP}_2, \ldots, \mathrm{AP}_N\}$ where the STA finds N APs, thereby $\mathrm{AP}_i \in U (1 \le i \le N)$. Then the STA performs the TFC and collects information about the achievable throughput (a_i) and RSSI (s_i) on every AP in the set U. The AP_i is assumed to have the maximum achievable throughput which is determined by

$$\arg\max_i a_i \in \left\{ i \forall j : a_j \le a_i \right\}, \tag{1}$$

and then the STA performs handoff to the AP_i.

When there exists more than one AP with the same maximum achievable throughput using (1), the AP selection algorithm employe the RSSI as another metric. Let $\overline{U}$ denote a set of APs, $\overline{U} = \{\mathrm{AP}_1, \mathrm{AP}_2, \ldots, \mathrm{AP}_M\}$, where M APs are determined with the same achievable throughput, thereby

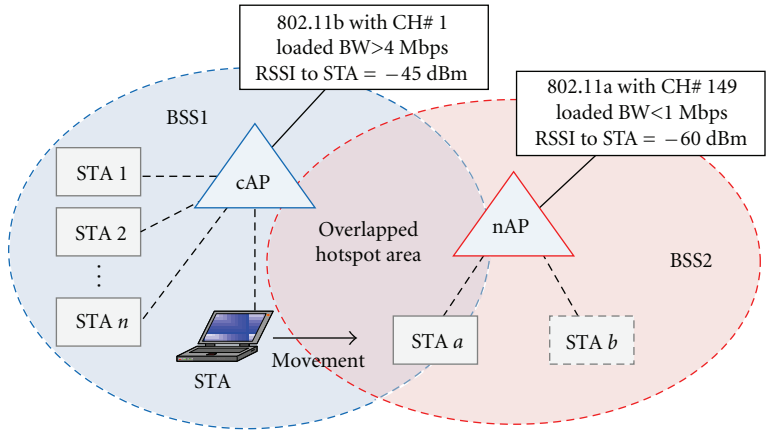

Figure 1: A scenario for MAC layer handoff within overlapped hotspot area.

$AP_i \in \overline{U}(1 \le i \le M \le N)$. As similar to (1), an optimal AP is determined by $\arg\max_i s_i$, and the STA finally performs to the AP_i which has the maximum a_i as well as s_i.

4. Transient Frame Capture

We mentioned that the proposed handoff mechanism utilizes the Transient Frame Capture (TFC) not only to estimate the bandwidth capacity of neighbor APs but also to predict the achievable throughput from the neighbor APs. Utilizing the TFC has several advantages as follows. (1) To the best of our knowledge, there exists no approach to passively measure the AP's bandwidth capacity and achievable throughput without any AP protocol change, and thus it can be easily applied to the any existing 802.11 NIC. (2) The TFC works with switching the NIC's operation status to a promiscuous mode during very short period, and thus it does not affect the current data service in use (The most of commercial IEEE 802.11 WLAN NIC supports to use the promiscuous operation by both kernel and user level API). (3) Measured information by utilizing the TFC can be used for estimating the achievable throughput from the neighbor APs and properly reflects wireless network environment which dynamically varies according to the link condition.

Figure 2 shows an example when an STA periodically performs the TFC to nAPs belonging to the BSS list which is collected by active scanning; for example, nAP1 and nAP2 work on channel number X' and X'', respectively. Each TFC procedure continues a certain time duration, Capture Period (CP). To minimize the service degradation of activated connection through cAP, the length of the CP should be as short as possible, but it affects the reliability of throughput estimation. The impact of the CP will be discussed in Section 6.1.

The detail procedure of a TFC is described as follows. Once an STA starts a TFC, it switches the channel of its NIC to the target channel of the nAP ($X \rightarrow X'$) and changes to the promiscuous mode to capture frames on the target channel. During a CP, the STA captures all WLAN frames and builds the nAP specific information based on a filtered

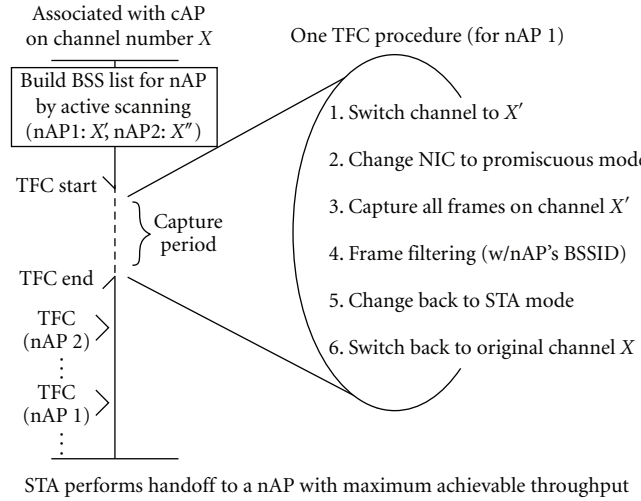

Figure 2: Transient frame capture.

set of frames whose sender or receiver address field in MAC header matches to the nAP's BSS Identification (BSSID). As soon as a CP expires, the TFC ends with changing the STA's mode back to the original (infrastructure mode) and switching the channel back to the original for the cAP ($X' \rightarrow X$). Since the TFC is conducted by fast channel switching within operating and nonoperating channels, STAs in range of several neighbor APs can obtain individual information of the APs even in a different channel. For neighbor APs in a same channel, STAs can collect the information by performing one TFC to the channel.

By utilizing the TFC, STAs can obtain several information, such as (sub)type, length, and Traffic Indication Map (TIM) fields from the MAC header of the captured frames. These pieces of information play an important role to infer the number of active STA which currently receives or transmits frames via the nAP, not the number of associated STA as in [14]. The number of active STA involved in receiving downlink frame from AP can be easily inferred by counting the receiver address field in downlink data frames.

Table 1: Parameter values for the analysis of throughput estimation.

Parameter	Values	Descriptions
ρ	20 μsec	A slot time
SIFS	10 μsec	Short Interframe Space
DIFS	50 μsec	Distributed IFS
ACK_TIMEOUT	300 μsec	ACK timeout
L_{PHY}	128 bits	PHY header length
L_{MAC}	272 bits	MAC header length
L_{ACK}	112 bits + L_{PHY}	ACK frame length
L	variable	Data length

However, a certain STA is activated but currently staying in power saving mode. We thus additionally address the TIM field in Beacon frames as to infer the number of receiving STA. Since the TIM includes a set of association ID of the STA whose downlink traffic is now buffered at the AP, counting 1 set bit denotes the number of active STA in receiving.

On the other hand, inferring the number of active STA involved in transmitting uplink frame to AP differs from that in receiving downlink frame because the STA cannot capture every frame on the target channel (X') because of following reasons. The first reason is that APs and STAs may drop frames if their internal buffer overflows. Fortunately, it is ignorable since we only focus our throughput estimation on the transmission rate of frames actually leaved from the APs or STAs. The other reason is that an STA is not in the propagation range of other STAs as known as hidden terminal. As an example, in Figure 1, the propagation range of nAP and STA a is reachable to the STA but that of STA b is not. It means that, by utilizing the TFC, the STA can capture only frames propagated from the nAP and the STA a, whereas it is impossible to capture any frame transmitted from the STA b. Therefore, we use the receiver address field in ACK frames to infer the number of active STA involved in transmitting uplink frame to the AP.

4.1. Implementation Issues. We implement a real-system testbed and demonstrate the TFC to estimate the bandwidth capacity and the achievable throughput from APs. The key part of the testbed implementation is the basis of the kernel level miniport driver for NIC in Realtek-8185 chipset under Microsoft Windows Vista's Network Driver Interface Specification (NDIS) architecture.

Figure 3(a) shows the overall architecture of the testbed where TFC functionalities are implemented as a capture module in the miniport driver. By calling the special function (DeviceIo-Control) from user application, the capture module starts the TFC procedure. While the TFC is performed, every frame captured on the specific channel is stored in Net Buffer List (NBL), and then the user application refers the captured frame by reading the address of the NBL as in Figure 3(b). Whenever the capture module performs a TFC procedure, it starts a timer for the Capture Period (CP timer) and saves the current context information such as the channel number and the operation mode of the NIC. As soon as the CP timer expires, the capture module restores to the original context information and finishes the TFC procedure.

5. Achievable Throughput Estimation

This section provides an analytic model to estimate the current bandwidth loaded on a target AP and to predict the achievable throughput which is expected after the STA associates with the AP. In addition, we also investigate the achievable throughput taking into account the rate discounted according to the wireless link condition, that is, RSSI and FER. Symbols for the analysis are explained in Table 1, and they will be used throughout this paper.

5.1. Bandwidth Capacity Estimation. Let n denote the number of active STA which is contending in an AP's BSS, and τ is the probability that an STA transmits in a given time slot. For a certain time slot, P_i, P_s, and P_c are the probability that the channel is idle, the transmission is successful because only one STA tries transmission, and the collision is occurred when more than two STAs simultaneously transmit, respectively, which are given by

$$\begin{aligned} P_i &= (1-\tau)^n, \\ P_s &= n \times \tau(1-\tau)^{n-1}, \\ P_c &= 1 - P_i - P_s. \end{aligned} \tag{2}$$

Let L_{PAYLOAD} and L_{UPPER} denote the length of a frame (payload) and upper layer protocol headers (i.e., IP and UDP), where $L = L_{\text{PAYLOAD}} - L_{\text{UPPER}}$. The average time associated with one successful transmission, T_s, and with collision, T_c, are given by

$$\begin{aligned} T_s &= T_{\text{PAYLOAD}} + T_{\text{PHY}} + T_{\text{MAC}} + T_{\text{ACK}} + \text{SIFS} + \text{DIFS}, \\ T_c &= T_{\text{PAYLOAD}} + T_{\text{PHY}} + T_{\text{MAC}} + \text{ACK\_TIMEOUT} + \text{DIFS}, \end{aligned} \tag{3}$$

where T_{PAYLOAD}, T_{ACK}, T_{PHY}, and T_{MAC} are the average time associated with the transmission of a payload, an ACK frame, a PHY header, and a MAC header, respectively. These can be easily obtained by dividing L_{PAYLOAD}, L_{ACK}, L_{PHY}, and L_{MAC} into the channel rate (CR) of the AP, respectively.

Based on (2) and (3), channel idle ratio (R_{idle}) and channel busy ratio (R_{busy}) can be expressed by

$$\begin{aligned} R_{\text{idle}} &= \frac{P_i \times \rho}{P_i \times \rho + P_s \times T_s + P_c \times T_c}, \\ R_{\text{busy}} &= 1 - R_{\text{idle}}. \end{aligned} \tag{4}$$

On substituting $L \times P_s$ for $P_i \times \rho$ in (4) we obtain the target AP's bandwidth, **B**, which is given by

$$\mathbf{B} = \frac{L \times P_s}{P_i \times \rho + P_s \times T_s + P_c \times T_c}. \tag{5}$$

By assuming that all data length is equal to L, R_{busy} can be derived from a function of n and τ. With the number of DATA frame (N_{DATA}) andACK frame (N_{ACK}) measured by

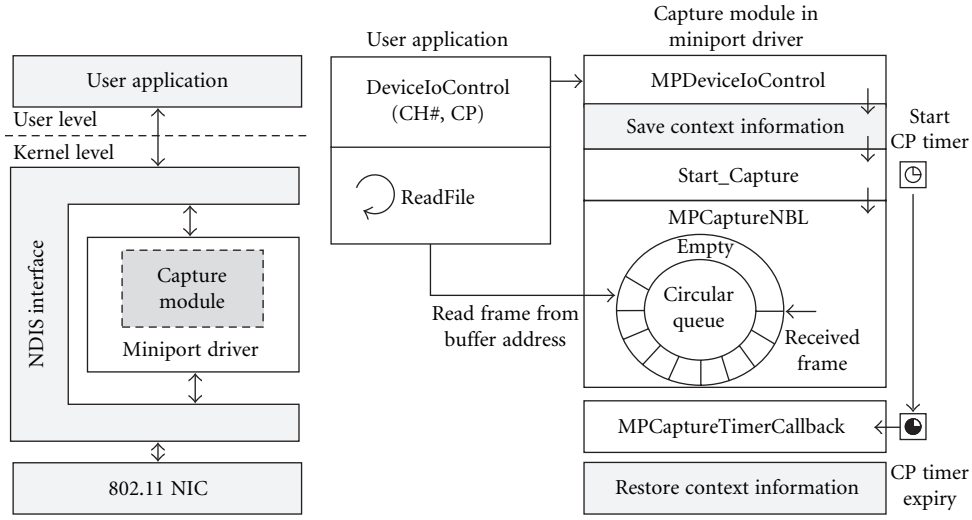

Figure 3: (a) Overall architecture of testbed implementation. (b) Work flows between user application and the capture module in the miniport driver.

the TFC, we can obtain the channel time associated with one successful transmission, T_s, for downlink and uplink traffic. Thus, for a CP, the busy ratio is given by $R_{\text{busy}} = ((N_{\text{ACK}} + N_{\text{DATA}}) \cdot T_s + (N_{\text{DATA}} - N_{\text{ACK}}) \cdot T_c)/\text{CP}$ where $N_{\text{DATA}} - N_{\text{ACK}}$ denotes the number of unacked data which is retransmitted during the channel collision, T_c. In addition, n is also inferred by the TFC as mentioned in Section 4. Based on the obtained R_{busy} and n, we can define τ as a nonlinear algebraic equation. Generally, the nonlinear algebraic equation can be exactly solvable through numerical method (e.g., Newton-Raphson method). Therefore, the AP's bandwidth ($\mathbf{B}$) can be made perfectly obtainable by using the (5).

Figures 4(a)–4(f) are plots of $\mathbf{B}$ by using (5) as a function of R_{busy} in $[0, 1]$ for the $L = 500$ and 1000 Bytes. Each analysis is computed by MATLAB programming when n is 1, 5, and 10, and CR is 1, 2, 5.5, and 11 Mbps. These results show that, for $n = 1$, the $\mathbf{B}$ has been increasing steadily as the R_{busy} increases, regardless of the L and the CR. On the other hand, for $n = 5$ and 10, the $\mathbf{B}$ has shown a linear increase until it reaches a local maximum, which denotes a saturated throughput, and decreases considerably as the R_{busy} increases.

5.2. Achievable Throughput Prediction. As we have seen in Section 5.1, STAs can estimate the bandwidth capacity currently loaded on the target AP by utilizing the TFC. However, the AP's bandwidth capacity does not indicate the throughput which is achievable after the STAs perform handoff to and associate with the AP. Therefore, we present how to predict the achievable throughput of APs based on the TFC we are addressing.

By using (4) and (5), we newly define $\mathbf{B}(n)$ and R^n_{busy} as the current bandwidth loaded on an nAP and its busy ratio, respectively, when the nAP has n active STAs. Then per-STA bandwidth in the nAP is given by $\mathbf{B}_n = \mathbf{B}(n)/n$ as a function of R^n_{busy}. Suppose that the number of active STA may increase to $n + 1$ when a new STA performs handoff and continues its transmission through the nAP. Thus we can expect the per-STA bandwidth in the nAP with $n + 1$ STAs as $\mathbf{B}_{n+1} = \mathbf{B}(n + 1)/(n+1)$. By assuming that every STA transmits (or receives) its individual traffic in same data rate within the nAP's range, $S(R^n_{\text{busy}})$ is the busy ratio for the maximum peak of $\mathbf{B}_n$, where $(d/dR^n_{\text{busy}})\mathbf{B}_n = 0$. It means that the throughput of the nAP with n-STA is saturated when $R^n_{\text{busy}} = S(R^n_{\text{busy}})$. Finally, an STA's achievable throughput, $\mathbf{A}$, from an nAP (i.e., the nAP with $n + 1$ STAs, but actually n STAs are associated with the nAP) is given by

$$\mathbf{A} = \begin{cases} (\mathbf{B}_{n+1}, \mathbf{B}_n] & \mathbf{B}_n \le \hat{\mathbf{B}}_{n+1}, \\ \left[0, \hat{\mathbf{B}}_{n+1}\right] & \left(\mathbf{B}_n > \hat{\mathbf{B}}_{n+1}\right) \wedge \left(R^n_{\text{busy}} \le S\left(R^{n+1}_{\text{busy}}\right)\right), \\ [0, \mathbf{B}_{n+1}) & \left(\mathbf{B}_n > \hat{\mathbf{B}}_{n+1}\right) \wedge \left(R^n_{\text{busy}} > S\left(R^{n+1}_{\text{busy}}\right)\right), \end{cases} \tag{6}$$

where $\hat{\mathbf{B}}_n$ is the maximum per-STA bandwidth from the nAP with n-STA when $R^n_{\text{busy}} = S(R^n_{\text{busy}})$. According to R_{busy}, the $\mathbf{A}$ has different ranges as follows. For $\mathbf{B}_n \le \hat{\mathbf{B}}_{n+1}$, the R_{busy} increases when the n becomes $n + 1$ since individual bandwidth occupied by each STA is same as $\mathbf{B}_{n+1}$. On the other hand, for $\mathbf{B}_n > \hat{\mathbf{B}}_{n+1}$, it is hard to estimate R^{n+1}_{busy} by using the TFC. Thus we choose zero as the lower bound of the $\mathbf{A}$. When $R^n_{\text{busy}} > S(R^{n+1}_{\text{busy}})$, the $\mathbf{A}$ may be less than $\mathbf{B}_{n+1}$ because the achievable throughput decreases as the busy ratio increases, while the $\mathbf{A}$ may be less than or equal to $\hat{\mathbf{B}}_{n+1}$ for $R^n_{\text{busy}} \le S(R^{n+1}_{\text{busy}})$. Figure 5 depicts the analysis result for the achievable throughput prediction when $n = 3$.

5.3. Rate Discount of Achievable Throughput. As an STA moves away from an AP, the signal from the AP reaches the STA with reduced power so that the lower RSSI is

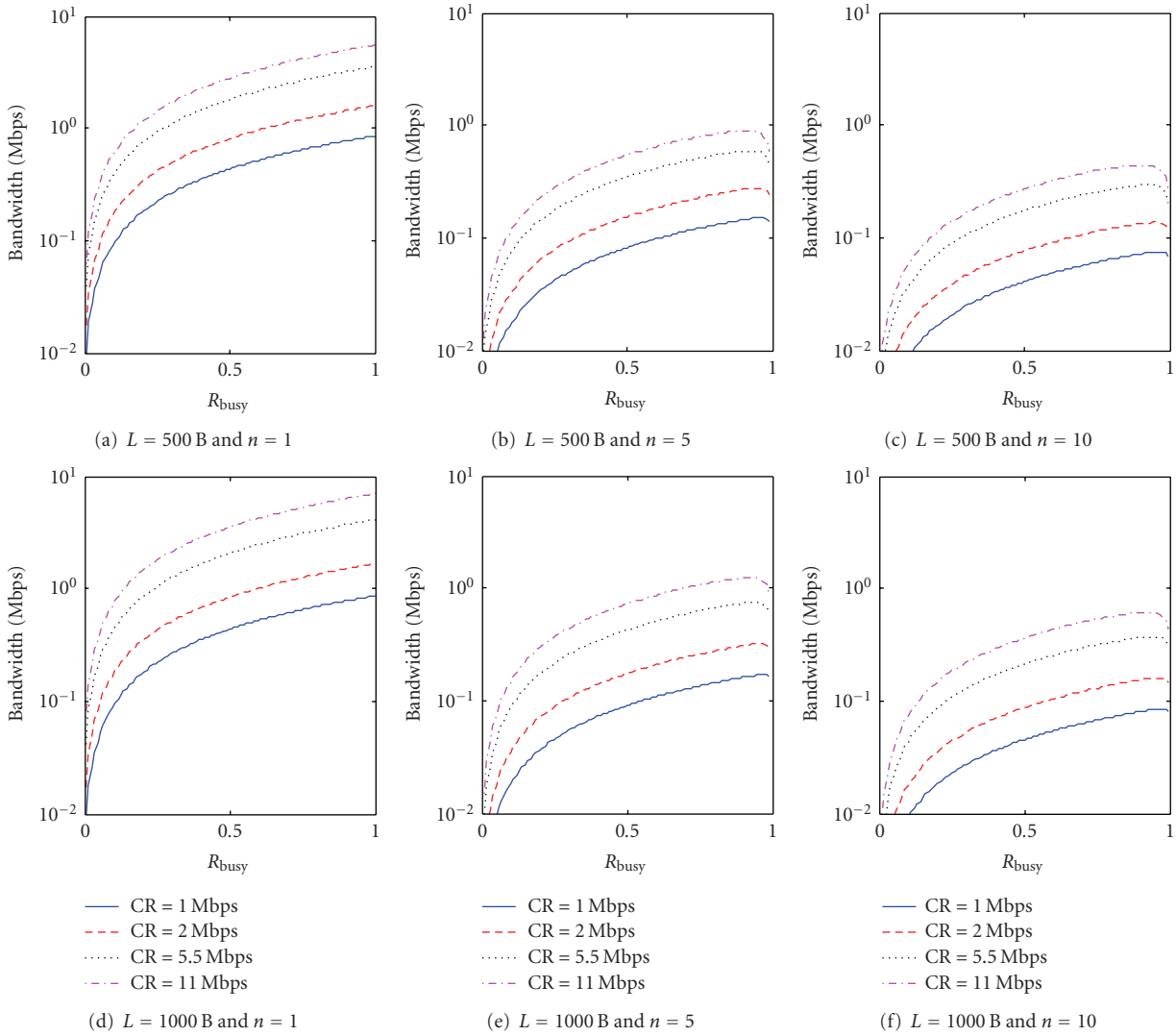

Figure 4: Numerical analysis results of bandwidth estimation.

measured at the STA. Even if an AP transmits a certain rate of data frames to an STA, the STA is likely to miss several frames because of frame loss or bit error occurrence in a poor wireless link condition. Typically, the lower RSSI is measured, and the STA suffers from the higher Bit Error Rate (BER), causing the degradation of the achievable throughput obtained from the AP. Therefore, the achievable throughput should be discounted according to the BER, and we call it rate discount. However, to the best of our knowledge, there exists no method to obtain the BER directly from the 802.11 NIC [17]. We thus present three alternative methods to obtain the discounted rate without the basis of the BER measurement.

5.3.1. Frame Retransmission versus RSSI. In 802.11, data frame loss or error initiates retransmission of the frame to provide reliable communications. As RSSI between STA and AP decreases, the number of frame retransmission may increase. Figure 6 shows the experiment result of frame retransmission ratio (ReTX) for CR in 1, 5.5, and 11 Mbps and average RSSI with respect to the distance between an STA and an 802.11b AP, from 10 m to 70 m at intervals of 7 meters. We generate 100 Kbps downlink traffic with 500 B length UDP datagram. The ReTX is calculated as # of retransmitted frame/# of received frame where the retransmitted frame is distinguished by *Retry* bit in 802.11 header. The result shows that the frame retransmission rarely occurs until 60 m (CR = 1), 50 m (CR = 5.5), and 40 m (CR = 11). After that, the frame retransmission ratio significantly increases, while the average RSSI gradually decreases as the distance increases. It means that we cannot determine the RSSI where the retransmission begins to increase regardless of the AP's channel rate. Even if the number of retransmitted frame is a good decision criterion for WLAN handoff [18], it is not applicable to obtain the discounted rate in our handoff mechanism since the STA cannot measure the number of frame retransmission without associating with the AP.

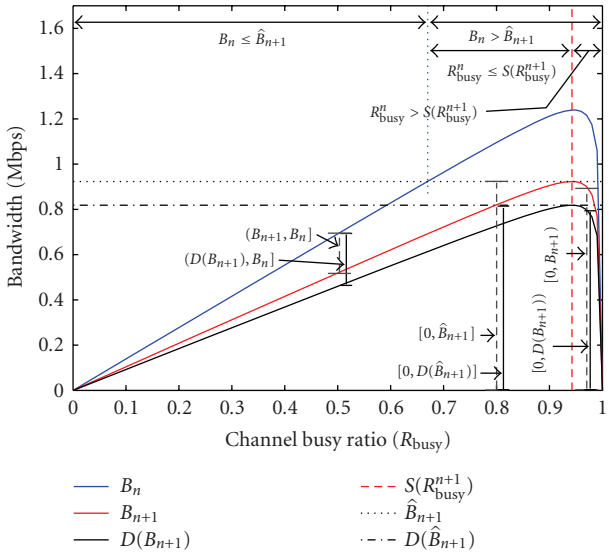

Figure 5: Numerical analysis of achievable throughput estimation /w and /wo rate discount for $n = 3$ and FER $= 0.1$.

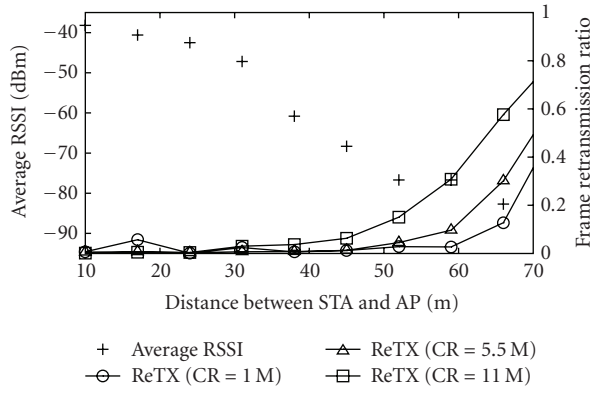

Figure 6: RSSI and frame retransmission ratio.

5.3.2. Throughput versus RSSI. When an AP transmits data frames to an STA at a constant rate, the receiving rate at the STA should be also constant. However, the receiving rate is determined by FER (regard it as related to BER); it thus varies according to signal conditions. BER is determined by Signal to Interference and Noise Ratio (SINR) where the signal is denoted by RSSI, but the noise cannot be obtained from the received signal. Since we are not intended to calculate exact rate value, the RSSI is still useful to deduce the discounted rate.

Figure 7 illustrates the experiment result of throughput and RSSI degradation as the distance between an STA and an AP increases where the AP is located at the start of an 80 m corridor whose width and height are 2 and 3 m, respectively. We plot the STA's throughput and RSSI for CR = 1, 2, 5.5, and 11 Mbps for 802.11b on channel 13 and CR = 6, 12, and 24 Mbps for 802.11a on channel 44 as the STA moves away from the AP and toward the end of the corridor at intervals of 2 meters until it reaches 80 m. During each experiment, a PC is directly connected to the AP in an Ethernet link and

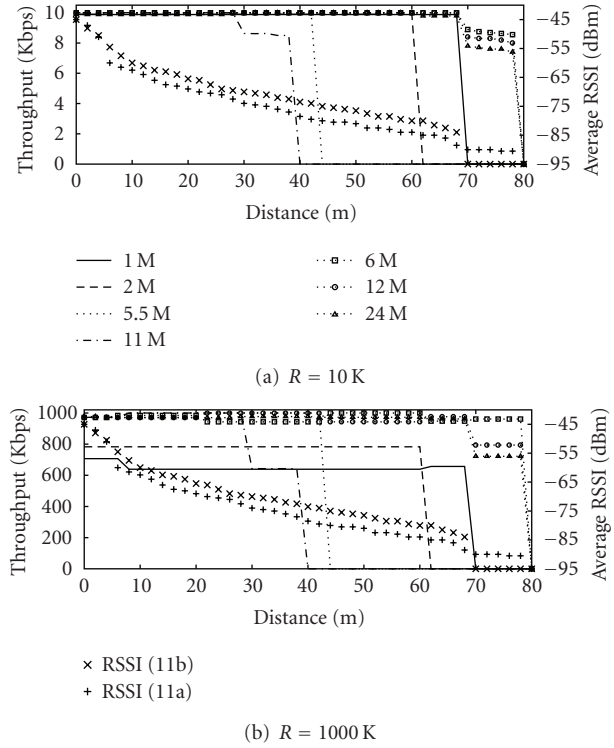

Figure 7: Throughput and RSSI versus distance.

generates traffic destined to the STA with a fixed rate (R) in 10 and 1000 Kbps. We use 1 KB length UDP datagram for the traffic generation.

The result shows that, for all R, the STA achieves less throughput as the distance increases. Furthermore, as R increases, the discounted rate is also increases regardless of CR. Remarkably, we can observe that the location where the throughput is dramatically decreased is similar as 68, 60, 44, and 28 m for CR = 1, 2, 5.5, and 11 Mbps (802.11b), and 70 m for CR = 6, 12, and 24 Mbps (802.11a). From these results, we believe that the discounted rate strongly depends on the RSSI and CR. Therefore, when the predicted achievable throughput of different APs is same, the comparison of the APs' RSSI is a useful metric to determine a better AP.

5.3.3. FER Measurement with Probe Frame. Usually the number of errors in a sequence of bits is modeled by a binomial distribution; thus FER can be expressed as FER $= 1 - (1 - \text{BER})^{L_{\text{DATA}}+L_{\text{ACK}}}$ where L_{DATA} is a DATA frame length [19]. Noting that the STA cannot send DATA frame to the not-yet-associated AP, we measure the FER by sending/receiving Probe Request/Response management frames instead of DATA/ACK frames. Since 802.11's contention mechanism for both management and DATA frames is same before being sent, the FER measurement with probe frames is acceptable. Let L_{P} denote the length of a pair of Probe Request and Response frame. (The IEEE 802.11 standard specifies that the Probe Request frame is broadcasted, but for the FER measurement, we

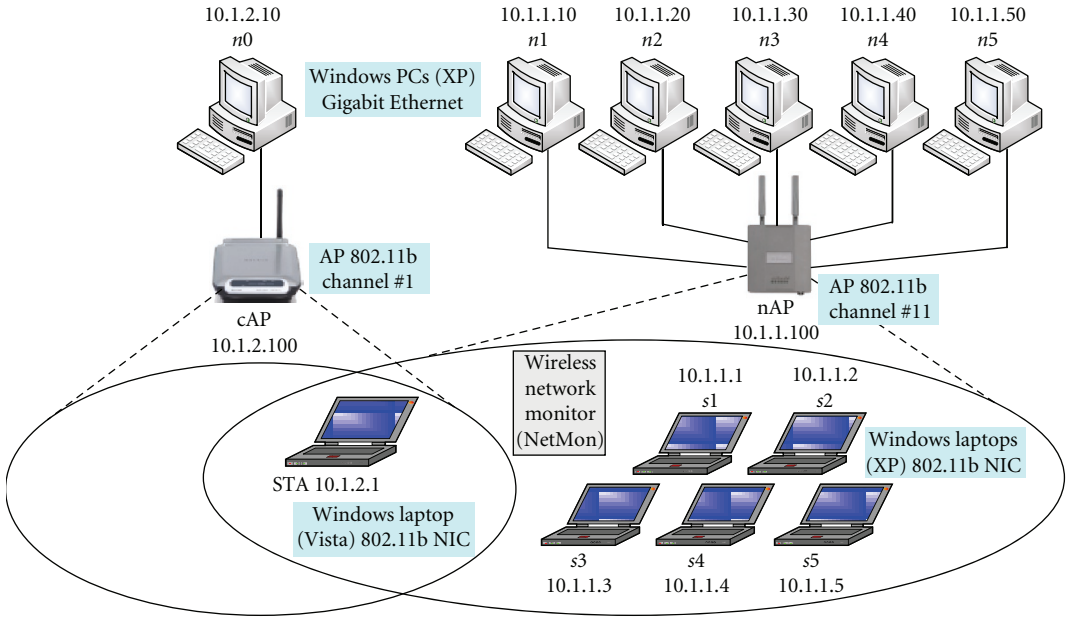

Figure 8: Experiment environment for throughput measurement with TFC.

used a unicast address as the destination address field of the Probe Request frame.) Then the probability of successful transmission for a pair of Probe Request and Response frames without error is given by $(1 - \text{BER})^{L_P}$, and it can be easily obtained by regarding the FER as 1−(# of received Probe Response/# of sent Probe Request). In addition, transmission may fail due to collision when the channel is congested. The probability of collisions occurred by other active STA can be expressed by $(1 - P_s - P_i)^{n-1} = (P_c)^{n-1}$ as introduced in [20] to increase the bandwidth accuracy. Hence, the rate discounted per-STA bandwidth achievable from the nAP with n-STA, $D(\mathbf{B}_n)$, is given by

$$D(\mathbf{B}_n) = \mathbf{B}_n \times (P_c)^{n-1} \times (1 - \text{BER})^{L_P}. \quad (7)$$

As an example, in Figure 5, we plot the range of $\mathbf{A}$ with rate discount by applying (7) for FER = 0.1 (black-solid error bar) when $n = 3$. Obviously, the range of $\mathbf{A}$ with rate discount differs from that of $\mathbf{A}$ without rate discount (gray-dashed error bar). The lower bound for $\mathbf{B}_n \leq \hat{\mathbf{B}}_{n+1}$ and the upper bound for $(\mathbf{B}_n > \hat{\mathbf{B}}_{n+1}) \wedge (R^n_{\text{busy}} > S(R^{n+1}_{\text{busy}}))$ are diminished in $D(\mathbf{B}_{n+1})$ since the throughput is affected by BER. On the other hand, for $(\mathbf{B}_n > \hat{\mathbf{B}}_{n+1}) \wedge (R^n_{\text{busy}} \leq S(R^{n+1}_{\text{busy}}))$, the upper bound is reduced to $D(\hat{\mathbf{B}}_{n+1})$.

6. Experimental Studies

This section provides the experiment of the proposed MAC layer handoff mechanism and the TFC. Figure 8 shows our experiment environment as follows. An STA works with a Windows Vista powered laptop equipping Netgear JWAG511 WLAN NIC and is associated with an 802.11b AP (cAP) on channel number 1. On the other hand, there exists a neighbor 802.11b AP (nAP) on channel number 11 which is orthogonal to that of the cAP. The nAP is a target to measure the achievable throughput by utilizing the TFC while the STA is connected via the cAP. The cAP and the nAP is deployed by using Belkin wireless b/g router and D-Link DWL-8200AP, respectively. The only modification is applied at the STA by installing implemented miniport driver.

In order to generate the cross traffic on the APs, we use Windows XP powered 6 PCs labeled from $n0$ to $n5$ and 5 laptops labeled from $s1$ to $s5$ as in Figure 8. While the $n0$ is connected directly to the cAP and generates the traffic destined to the STA, other PCs ($n1 \sim n5$) are directly connected to the nAP and generate the traffic destined to the corresponding laptops ($s1 \sim s5$). Additionally, we locate a PC with a tool provided by [21], namely, NetMon, on near by the nAP. The NetMon is to capture every frame transmitted from the nAP, thus works independently of others. To simplify, we assume that every PC generates their traffic with fixed-length UDP datagram, and the direction of the traffic is downlink. For the experiment of the traffic in uplink direction, we could obtain similar results as the downlink traffic experiment.

6.1. Impact of Capture Period (CP). In regards to the throughput measurement, finding an optimal CP plays an important role to make the TFC procedure do not disrupt the active session via the associated cAP. We thus do an experiment to find the optimal CP which minimizes the data loss of the current active session. The $n0$ sends the traffic of 1000-Byte length UDP datagram generated with 20 milliseconds interval (= 400 Kbps), and we check the sequence number of each datagram. (We implement a new traffic generation application that the sequence number is appeared in the data part of each UDP datagram.) As a result, we observe that no data loss is examined when CP $\leq$ 200

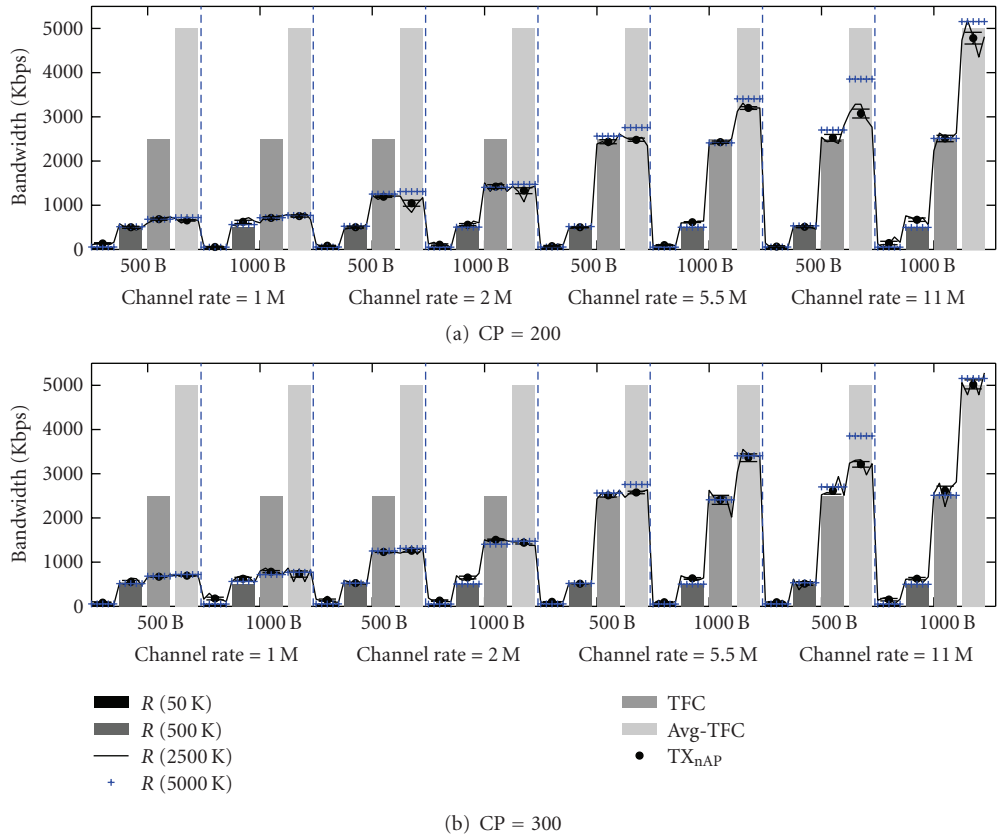

FIGURE 9: Case 1: comparison between estimated bandwidth with the TFC and AP's actual transmission rate (TX_{nAP}) for $n = 5$.

milliseconds, while for CP = 300 milliseconds, the result averaged over 10 experiments shows that 1.8 datagrams are lost during a TFC procedure. However, if the CP $\geq$ 400 milliseconds, the number of datagram loss is significantly increased in average 3.4 and 5.7 for CP = 400 and 500 milliseconds, respectively.

We confirmed that the datagram is lost since the STA cannot receive frames sent from the cAP while the STA is in the promiscuous mode for the TFC procedure. When the cAP does not receive ACK for a sent frame, it sends the frame again until exceeding the retransmission limit in *RetryLimit* where the *RetryLimit* is usually set by 7, but it is dependent to the NIC manufacturer. After the number of retransmission exceeds the *RetryLimit*, the cAP drops the frame and tries to send the other frame in its buffer. In the rest of experiments, we thus use two CPs of 200 and 300 milliseconds to improve the reliability of data transmissions via the cAP during the TFC proceeds.

It is worth noting that the selection of CP duration is a huge problem since the heuristic value of the CP may not fit other network setups. We thus address a method to avoid the service degradation of data connection through the associated cAP. Whenever an STA performs a TFC to the other channel for nAPs, it employs power saving technique as follows.: Before the STA switches its channel to a target AP's channel, it sends a null frame to the cAP, which is to enter into the power saving mode. During a CP for the TFC, the cAP buffers data destined to the STA and informs it via TIM at beacon frame by next listen interval. As soon as the STA switches back to the original channel on the cAP, it sends PS-POLL frame to the cAP and then receives the buffered data from the cAP.

6.2. Evaluation. We evaluate the performance of the TFC on (1) reliable and (2) accurate estimation of AP's bandwidth capacity by studying experiments in various traffic environments. Also, we show that the prediction of the achievable throughput, which is the basis of the estimated bandwidth capacity, well matches the actual throughput from the AP even applying (3) rate discount based on the FER measurement.

Each of these evaluation cases are performed under individual experiment scenario. During each experiment scenario, we apply different n's; thus, according to the n, n PCs send UDP datagram in L = 500 and 1000 B destined to the corresponding n laptops with the rate in 10, 100, 500, and 1000 Kbps to generate cross traffic on the nAP. Also, we vary the nAP's CR in 1, 2, 5.5, and 11 Mbps and the CP for the TFC in 200 and 300 milliseconds for various traffic environments.

6.2.1. Case 1—Reliable Bandwidth Estimation. Figures 9(a) and 9(b) are plots of the estimated bandwidth loaded on the nAP (TFC) as a function of cross traffic when five other STAs

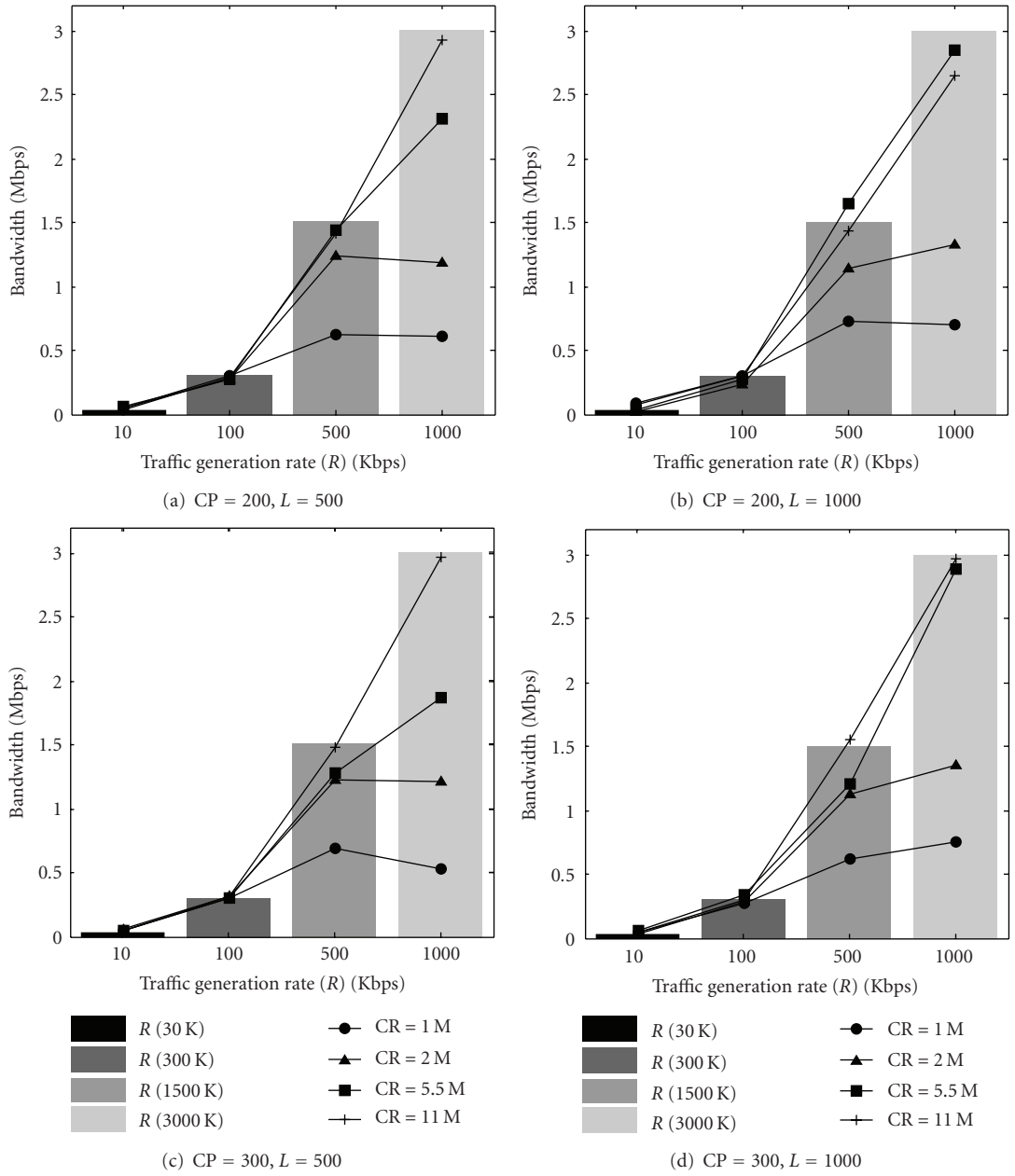

Figure 10: Case 2: estimated bandwidth in average with the TFC for $n = 3$.

receive downlink traffic from the nAP ($n = 5$) and CR = 1, 2, 5.5, and 11 Mbps for CP = 200 and 300 milliseconds, respectively. We generate 10, 100, 500, and 1000 Kbps of cross traffic from each of five PCs ($n1 \sim n5$). For the nAP, this cross traffic is denoted as reference bandwidth in R(50 K), R(500 K), R(2500 K), and R(5000 K), respectively. For each traffic scenario, the nAP's bandwidth is estimated by utilizing the TFC at the STA. The estimated bandwidth averaged over 5 TFC trials (Avg-TFC) with standard error is compared with the reference bandwidth. We also compare the estimated bandwidth (TFC) with the nAP's actual transmission rate (TX_{nAP}) obtained by an independent NetMon (see Figure 8).

As a result, we can obtain that the reference bandwidth differs from the TX_{nAP}. When CR is lower than the reference bandwidth (i.e., R(2500 K) and R(5000 K) for CR $\leq$ 2 Mbps), the actual bandwidth on the nAP is lower than the reference bandwidth since the nAP cannot transmit all traffic flowed from PCs ($n1 \sim n5$) to laptops ($s1 \sim s5$) with the configured channel rate. It means that comparing the estimated bandwidth with the TX_{nAP} is more reliable. Most of the result indicates that the estimated bandwidth with the TFC is well matched to the TX_{nAP} rather than the reference bandwidth. Moreover, the standard error of 5 TFC trials is distributed within the reliable range of the actual bandwidth loaded on the nAP.

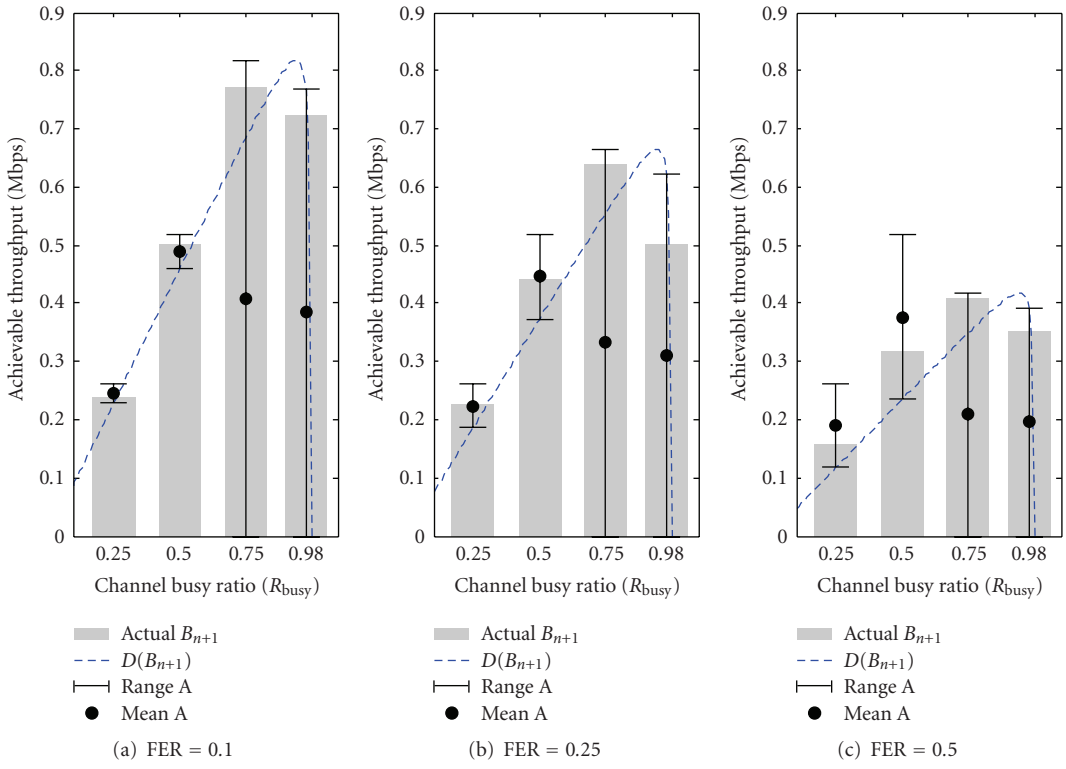

Figure 11: Case 3: achievable throughput estimation for $n = 3$ & CR = 5.5 Mbps.

Remarkably, in the case of R(500 K) for CR = 11 Mbps and L = 500 B, the TFC measurement underestimates the bandwidth on the nAP. Because the nAP receives five types 1 Mbps traffic with short L from PCs ($n1 \sim n5$), it heavily increases the nAP's transmission rate, and the STA cannot capture all the frame transmitted from the nAP. This problem can be solved if the STA uses large enough CP for utilizing the TFC procedure, but the large CP may degrade the service through the current associated cAP as mentioned in Section 6.1.

As an additional observation, the TX_{nAP} is higher than the reference bandwidth when the CR = 11 Mbps and L = 1000 B for both CP = 200 and 300 milliseconds. This is caused by the nAP's retransmission of data frames when the nAP does not receive corresponding ACK frame before the ACK_TIMEOUT expires.

6.2.2. Case 2—Accuracy of Bandwidth Estimation. Figures 10(a), 10(b), 10(c), and 10(d) are plots of the estimated bandwidth in average of 5 TFC trials as a function of traffic generation rate (R) when CR = 1, 2, 5.5, and 11 Mbps for (CP = 200, L = 500), (CP = 200, L = 1000), (CP = 300, L = 500), and (CP = 300, L = 1000), respectively. In this experiment, three PCs ($n1$, $n2$, and $n3$) generate UDP datagram with the R of 10, 100, 500, and 1000 Kbps for cross traffic on the nAP ($n = 3$); thus the reference bandwidth to be compared with the estimated bandwidth is R(30 K), R(300 K), R(1500 K), and R(3000 K), respectively. Most of the result shows that the estimated bandwidth increases as higher traffic is loaded on the nAP. However, several results of the estimated bandwidth for R = 500 Kbps are higher than thos for R = 1000 Kbps when CR $\leq$ 2 Mbps and L = 500, because the CR is lower than the traffic generation rate. The other reason why these results happen is that the UDP datagram length of the cross traffic affects the nAP's processing overhead where the shorter L makes data frames on the nAP be generated with the more frequent interval. Thus the accurate bandwidth estimation should take into account the current channel rate set on both the nAP and the STA. The rest of the results show that the bandwidth estimation with the TFC matches in higher accuracy when the CR is greater than the reference bandwidth.

6.2.3. Case 3—Achievable Throughput Prediction with Rate Discount. In Cases 1 and 2, we evaluated how well measured actual nAP's bandwidth capacity by utilizing the TFC. In Case 3, we investigate the prediction of the achievable throughput based on the nAP's bandwidth estimated by the TFC. Figures 11(a), 11(b), and 11(c) are plots of the achievable throughput predicted by (6) as a function of R_{busy} for FER = 0.1, 0.25, and 0.5, respectively, when the CR = 5.5 Mbps on the nAP. In this experiment, we perform the TFC for $n = 3$ on the nAP; thus it is to predict the achievable throughput (range **A**) from the nAP for $n = 4$ which is expected after the STA associates with the nAP. To simplify the experiment, we generate cross traffic in fixed length (L = 1000 B) and adjust R_{busy} in 0.25, 0.5, 0.75, and 0.98 by varying the individual traffic generation rate in PCs. We first measure the nAP's bandwidth capacity ($\mathbf{B}_n$) with the TFC when three PCs ($n1 \sim n3$) generate traffic destined to

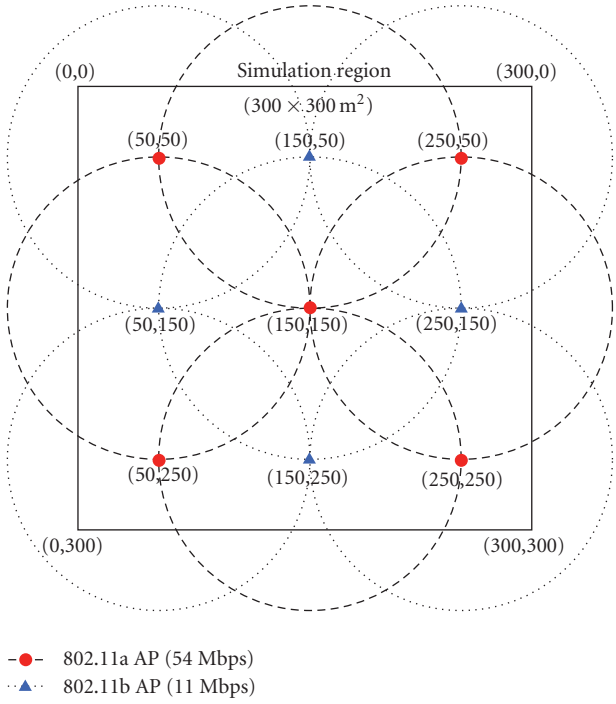

Figure 12: Simulation environment.

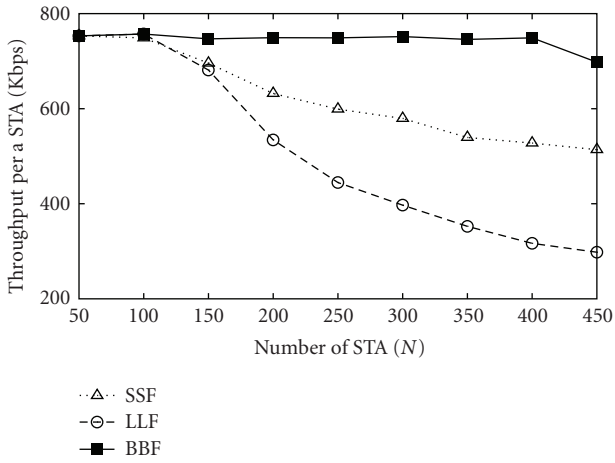

Figure 13: Average throughput per an STA.

the corresponding three laptops ($s1 \sim s3$). Then we make an STA associate with the nAP for the nAP in $n = 4$ and measure the actual throughput (actual $\mathbf{B}_{n+1}$) obtained from the nAP when $n0$ sends UDP traffic to the STA through the nAP.

For the same R_{busy}, the achievable throughput decreases as FER increases since it is affected by the quality of channel condition. Remarkably, comparing the rate discounted per-STA bandwidth obtained by (7) ($D(\mathbf{B}_{n+1})$) with the actual $\mathbf{B}_{n+1}$ leads to a similar bound. Also, every actual $\mathbf{B}_{n+1}$ is appeared within the range of $\mathbf{A}$. Especially, for $R_{\text{busy}} \leq 0.5$, we can observe that the actual $\mathbf{B}_{n+1}$ is closely distributed around the mean $\mathbf{A}$. In contrast, for $R_{\text{busy}} > 0.5$, the actual $\mathbf{B}_{n+1}$ is also appeared within the range of $\mathbf{A}$, but it is distributed in much more closer to the upper bound of the $\mathbf{A}$.

Table 2: Simulation parameters.

Parameter	Value
Simulation region	$300 \times 300\,\text{m}^2$
The number of AP	9
AP's channel rate	11 and 54 Mbps (Fixed)
AP's transmission range	100 m radius
The number of STA (N)	$50 \sim 450$
Required bandwidth by a STA	$500 \sim 1000$ Kbps

6.3. Fairness. The proposed handoff mechanism also fairly balances the traffic loaded on multiple APs in regard to their bandwidth capacity. With a simple simulation in C programming, we evaluate the fairness of traffic load distributed on the APs by comparing our proposed mechanism, namely Best Bandwidth Fit (BBF), with two conventional AP selection mechanisms [22], Strongest Signal First (SSF) and Least Load First (LLF). The SSF and the LLF triggers STAs to perform handoff to an AP with the strongest signal strength and the lowest traffic load, respectively. In the BBF, on the other hand, STAs perform handoff to an AP with the most bandwidth capacity obtained by TFC so that it takes into account both the achievable throughput and the signal strength from the AP.

We use simulation parameters as in Table 2. As shown in Figure 12, within the simulation region, we deploy 9 APs in the fixed location with different channel rates (five 802.11a and four 802.11b APs) and set all their channels which do not interfere one another. By setting that the AP's propagation range is 100 m, every STA can sense the carrier from at least one AP up to four overlapped APs. We vary the number of STAs (N) from 50 to 450 where each STA locates in random location within the simulation region and requires constant bandwidth chosen from 500 to 1000 Kbps (average 750 Kbps). Each simulation is performed 10 times and obtained the result in average.

6.3.1. Throughput per an STA. Figure 13 shows the average achieved throughput per an STA for SSF, LLF, and BBF mechanisms as N increases. When $N > 150$, SSF and LLF dramatically decrease the throughput per an STA since they force the STAs to select an AP according to only the signal strength and the amount of loaded traffic. On the other hand, BBF mechanism does not fluctuate the throughput per an STA since it fairly distributes the bandwidth capacity on the APs.

6.3.2. AP's Bandwidth Utilization. Figure 14 depicts the average bandwidth utilization on APs as a function of N. When $N > 150$ which denotes that 802.11b APs are saturated, STAs in LLF mechanism are likely to select 802.11b APs since the loaded traffic on the 802.11b APs ($\leq$11 Mbps) is less than that on the 802.11a APs ($\leq$54 Mbps) so that the utilization remains in about 60%. On the other hand, the average utilization of APs in SSF and BBF mechanism shows a linear growth. It means that APs in different PHY types fully utilize their bandwidth capacity as the number of STA increases.

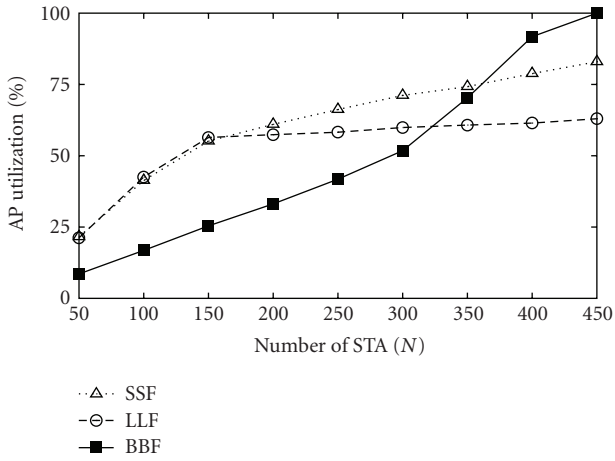

Figure 14: Average bandwidth loaded on an AP.

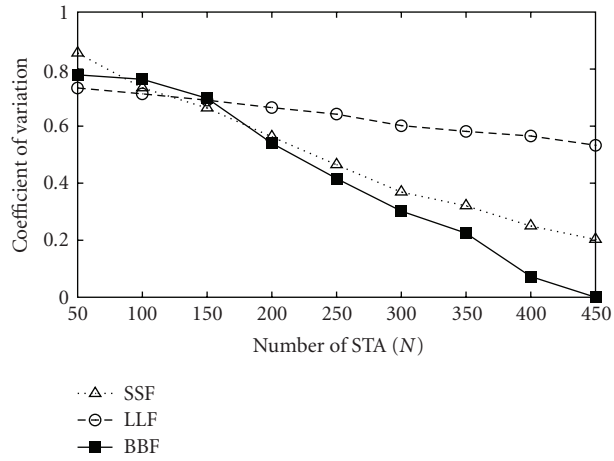

Figure 15: CV of AP's traffic load.

6.3.3. Coefficient of Variation. In order to show the fairness of traffic distribution on APs, we obtained the coefficient of variation (CV) in regard to the traffic loaded on the APs. The CV is calculated by CV $= \sigma/\mu$ where σ and μ are the standard deviation and the mean of the loaded traffic for all APs. Figure 15 is a plot of the CV as a function of the number of STA. As N increases, the CV of every mechanism is gradually reduced. The reducing slope of LLF mechanism is slight while those of SSF and BBF mechanisms are drastically reduced. After the 802.11b APs are saturated ($N > 150$), the CV of BBF mechanism is less than that of SSF mechanism. It is obvious that BBF mechanism can more fairly distribute the traffic load on densely deployed APs than other mechanisms.

7. Conclusion

In this paper, we proposed a MAC layer handoff mechanism for IEEE 802.11 WLAN to determine an optimal AP with the maximum achievable throughput rather than the highest RSSI. The proposed handoff mechanism performs Transient Frame Capture (TFC) to estimate the neighbor AP's bandwidth capacity and achievable throughput without service degradation of the active connection through the current associated AP. Based on the numerical analysis and experimental studies, we showed that the estimation result of analytical model reasonably well matches the empirical one in terms of reliable and accurate bandwidth capacity as well as rate discounted achievable throughput from neighbor APs. The proposed handoff mechanism also achieves a better fairness by balancing the traffic load on the densely deployed APs. Moreover, our mechanism requires no changes in AP protocols; thus it is easily applicable to any IEEE 802.11 WLAN NIC-based STA.

As a future work, we will study a further model for throughput estimation taking into account the dynamic length of L which was assumed as a fixed length in this paper. In addition, we assumed that APs use fixed channel rate, but the APs are often set with automatic fallback algorithm to dynamically adjust the rate against the distance between STAs and the APs. Thus the heterogeneity of channel rate in APs should be considered to design the estimation model.

Acknowledgments

This work was in part supported by a grant from Microsoft Research Asia. This work was also partially supported by the Korea Science and Engineering Foundation (KOSEF) grant funded by the Korea government (MEST) (2009-0076476).

References

[1] "IEEE Std 802.11. Wireless LAN Medium Access Control (MAC) and Physical Layer (PHY) Specifications," 1997.

[2] V. Mhatre and K. Papagiannaki, "Using smart triggers for improved user performance in 802.11 wireless networks," in *Proceedings of the 4th International Conference on Mobile Systems, Applications and Services (MobiSys '06)*, pp. 246–259, Uppsala, Sweden, June 2006.

[3] I. Ramani and S. Savage, "SyncScan: practical fast handoff for 802.11 infrastructure networks," in *Proceedings of the 24th Annual Joint Conference of the IEEE Computer and Communications Societies (INFOCOM '05)*, vol. 1, pp. 675–684, Miami, Fla, USA, March 2005.

[4] H. Wu, K. Tan, Y. Zhang, and Q. Zhang, "Proactive scan: fast handoff with smart triggers for 802.11 wireless LAN," in *Proceedings of the 26th IEEE International Conference on Computer Communications (INFOCOM '07)*, pp. 749–757, Anchorage, Alaska, USA, May 2007.

[5] V. Brik, A. Mishra, and S. Banerjee, "Eliminating handoff latencies in 802.11 WLANs using multiple radios: applications, experience, and evaluation," in *Proceedings of the ACM SIGCOMM Internet Measurement Conference (IMC '05)*, pp. 299–304, 2005.

[6] C. Dovrolis, P. Ramanathan, and D. Moore, "Packet-dispersion techniques and a capacity-estimation methodology," *IEEE/ACM Transactions on Networking*, vol. 12, no. 6, pp. 963–977, 2004.

[7] K. Lakshminarayanan, V. N. Padmanabhan, and J. Padhye, "Bandwidth estimation in broadband access networks," in *Proceedings of the ACM SIGCOMM Internet Measurement Conference (IMC '04)*, pp. 314–321, 2004.

[8] S. Vasudevan, K. Papagiannaki, C. Diot, J. Kurose, and D. Towsley, "Facilitating access point selection in IEEE 802.11

wireless networks," in *Proceedings of the ACM SIGCOMM Internet Measurement Conference (IMC '05)*, p. 26, 2005.

[9] M. Li, M. Claypool, and R. Kinicki, "Packet dispersion in IEEE 802.11 wireless networks," in *Proceedings of Conference on Local Computer Networks (LCN '06)*, pp. 721–729, 2006.

[10] A. Bazzi, M. Diolaiti, C. Gambetti, and G. Pasolini, "WLAN call admission control strategies for voice traffic over integrated 3G/WLAN networks," in *Proceedings of the 3rd IEEE Consumer Communications and Networking Conference (CCNC '06)*, vol. 2, pp. 1234–1238, 2006.

[11] D. Pong and T. Moors, "Call admission control for IEEE 802.11 contention access mechanism," in *Proceedings of IEEE Global Telecommunications Conference (GLOBECOM '03)*, vol. 1, pp. 174–178, San Francisco, Calif, USA, December 2003.

[12] Z. Kong, D. H. K. Tsang, and B. Bensaou, "Measurement assisted model-based call admission control for IEEE 802.11e WLAN contention-based channel access," in *Proceedings of the 13th IEEE Workshop on Local and Metropolitan Area Networks (LANMAN '04)*, pp. 55–60, April 2004.

[13] S. Kandula, K. C.-J. Lin, T. Badirkhanli, and D. Katabi, "FatVAP: aggregating AP backhaul capacity to maximize throughput," in *Proceedings of the 5th USENIX Symposium on Networked Systems Design and Implementation (NSDI '08)*, pp. 89–104, San Francisco, Calif, USA, April 2008.

[14] "IEEE Std 802.11e. Wireless LAN Medium Access Control (MAC) and Physical Layer (PHY) Specifications, Amendment 8: Medium Access Control (MAC) Quality of Service Enhancements," 2005.

[15] "IEEE Std 802.11k. Wireless LAN Medium Access Control (MAC) and Physical Layer (PHY) Specifications, Amendment 1: Radio Resource Measurement of Wireless LANs," 2008.

[16] S. Mangold and L. Berlemann, "IEEE 802.11k: Improving confidence in radio resource measurements," in *Proceedings of the 16th IEEE International Symposium on Personal, Indoor and Mobile Radio Communications (PIMRC '05)*, vol. 2, pp. 1009–1013, Berlin, Germany, September 2005.

[17] A. F. Conceicao, J. Li, D. A. Florencio, and F. Kon, "Is IEEE 802.11 ready for VoIP?" in *Proceedings of the 8th IEEE Workshop on Multimedia Signal Processing (MMSP '06)*, pp. 108–113, October 2007.

[18] K. Tsukamoto, T. Yamaguchi, S. Kashihara, and Y. Oie, "Experimental evaluation of decision criteria for WLAN handover: signal strength and frame retransmission," *IEICE Transactions on Communications*, vol. E90-B, no. 12, pp. 3579–3590, 2007.

[19] Y. Y. Kim and S.-Q. Li, "Modeling multipath fading channel dynamics for packet data performance analysis," *Wireless Networks*, vol. 6, no. 6, pp. 481–492, 2000.

[20] D.-J. Deng, C.-H. Ke, H.-H. Chen, and Y.-M. Huang, "Contention window optimization for IEEE 802.11 DCF access control," *IEEE Transactions on Wireless Communications*, vol. 7, no. 12, pp. 5129–5135, 2008.

[21] Microsoft, "Network Monitor 3.1," http://blogs.technet.com/netmon.

[22] Y. Bejerano, S.-J. Han, and L. Li, "Fairness and load balancing in wireless LANs using association control," *IEEE/ACM Transactions on Networking*, vol. 15, no. 3, pp. 560–573, 2007.